DARK CRATER-RELATED DEPOSITS ON VENUS IN RADAR CROSS-SECTION – EMISSIVITY DOMAIN.
N. V. Bondarenko[1,2], [1]Institute of Radiophysics and Electronics, National Academy of Science of Ukraine, 12 Ak.Proskury, Kharkov, 61085, Ukraine; [2]Dept. Geol. Sci., Brown University, Providence RI, USA. natasha@mare.geo.brown.edu.

Introduction: The population of Venus impact craters is rather small (about 1000). About 10% of all craters have distinctive associated dark diffuse features (DDF) like parabolas or halos. Such craters are thought to be the youngest on the planet [1,2]. The DDF are interpreted as surface deposits of loose material (dust) formed by the impact. DDF change their form with geological time and disappear due to eolian activity, which moves the dust and scatters it over large areas, and/or due to some weathering processes [3]. In [4] the morphological degradation stage of DDF was used to arrange the craters according to their relative age.

The objective of this work is the study of DDF material and processes of its evolution with the radiophysical properties of the DDF.

Approach and general observations: Data of Magellan radar experiment in active and passive modes were used. C1-MIDR mosaics were used as a source of SAR radar cross-section σ data and emissivity maps (GEDR data set) to get the emissivity values *E*. Spatial resolution of SAR data was decreased to make it comparable to GEDR maps. Data from the first cycle of Magellan survey were used.

Surroundings of craters with diameters of 30 – 80 km were studied. There are 91 craters with DDF in the low-latitude zone. The set includes 21 "dark parabola" craters (DP), 39 "clear dark halo" craters (CDH), and 31 "faint dark halo" craters (FDH), according to classification from [4].

Three general observations were made.

(1) The range of *E* values of DDF is narrower in comparison to the surroundings. The DDF material is more homogeneous in comparison to the diversity of the surrounding surface units.

(2) The radar contrast (the difference in the radar cross-section) between the DDF and the surrounding surface is rather high for DP craters, lower for CH craters, and even lower for FH craters.

(3) For 57 craters, areas with a gradual change of radar brightness and nearly constant emissivity were found. These areas have different size and shape, but they are always associated with DDF. An example of such a feature for crater Ban Zhao (17.2°N, 146.9°E) is presented in **Fig. 1**. **Fig.1a** shows SAR image (σ), **Fig.1b** - emissivity *E* for the same region. σ-*E* diagram for the area is presented in **Fig. 2**. Crosses in **Fig. 1** and **Fig. 2** show how observed properties vary across the feature.

Rather distinctive "emissivity" features were found for every DP craters (with 2 exceptions due to rough surface masked the emissivity changing), 20 CDH and 18 FDH craters.

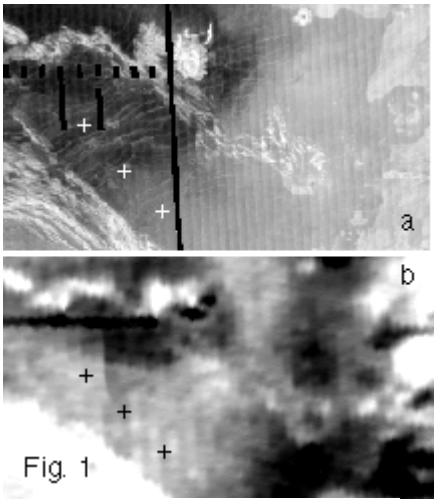

Fig. 1

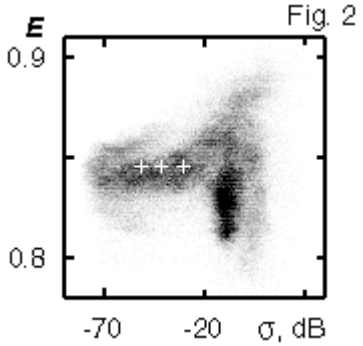

Fig. 2

Model for radiophysical properties of mantled surface. Possible properties of mantles from the impact event were studied with simple model of surface structure: a halfspace of material with dielectric permittivity ε_S representing the substrate covered by a mantle with dielectric permittivity ε_M. We considered that space-mantle interface is flat and for mantle – substrate interface the Kirchhoff approximation [5] can be used.

The backscattering coefficient for the model is

$$\sigma(q) = C \cdot A \cdot B(\varepsilon_M, q) \cdot B(\frac{1}{\varepsilon_M}, q'),$$

where factor *C* denotes backscattering coefficient from the substrate [5]:

$$C = \left[\left| R(\frac{\varepsilon_S}{\varepsilon_M}, 0) \right|^2 \exp(-\tan^2 q' / 2x^2) \right] \Big/ \left[2x^2 \cos^4 q' \right],$$

where $R(\varepsilon,\theta)$ is the Fresnel reflection coefficient at the incident angle θ for corresponding dielectric permittivity for interface ε, ξ is the *rms* slope of the substrate, θ is the incident angle of radiation, and θ' is the incident angle of radiation in the mantle material. Factor A presents the attenuation of the radiation during passage through the mantle:

$$A = \exp(-4\pi \cdot \tan\Delta \cdot \sqrt{\varepsilon_M} \cdot H \cdot \cos\theta' / \lambda),$$

where λ is the wavelength, $\tan\Delta$ and ε_M are the loss tangent and dielectric permittivity of the mantle material, and H is the mantle thickness. Factor B is equal to $B(\varepsilon,\theta) = \left[1 - |R(\varepsilon,\theta)|^2\right]$ and denotes the proportion of radiation passing through an interface.

The emissivity in the model was calculated as $E(\theta) = 1 - \Gamma(\theta)$, where $\Gamma(\theta)$ is reflectivity at the angle of observation θ. Reflectivity includes radiation reflected at the upper interface and that scattered by the lower interface into the upper halfspace through the mantle.

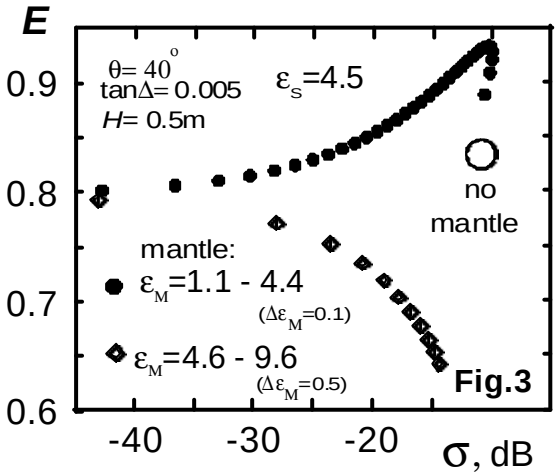

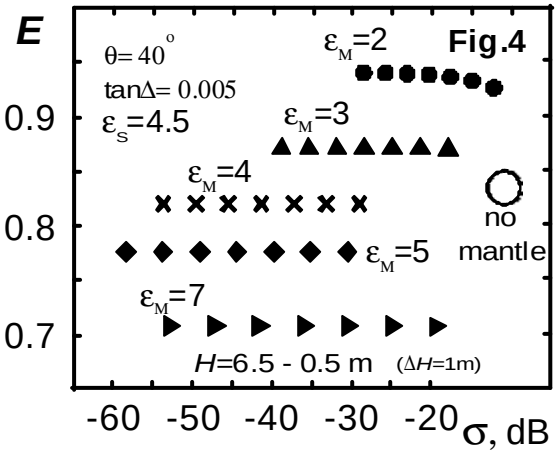

Some calculation results are shown in **Fig.3** and **Fig. 4**. The substrate with dielectric permittivity of 4.5, *rms* slope of 0.25, mantle material loss tangent of 0.005, and the observation angle of 40° were considered. Calculations presented in **Fig. 3** were made for the mantle thickness of 0.5 m and two ranges of mantle permittivity: 1.1 through 4.4 by 0.1 (dots), and 4.6 through 9.6 by 0.5 (rhombs). In the first case, the rightmost dot corresponds to the mantle permittivity of 1.1. The rightmost rhomb corresponds to the mantle permittivity of 9.6.

Influence of the mantle thickness on radiophysical properties is shown in **Fig. 4** for mantle permittivity of 2, 3, 4, 5, and 7. The mantle thickness varies here from 0.5 to 6.5 m. Circles in **Fig. 3** and **Fig. 4** mark the location of the surface without mantle in the radar cross-section – emissivity domain.

Fig. 3 and **Fig. 4** show that the presence of the mantle alters radar cross-section and emissivity. The emissivity is most sensitive to dielectric permittivity of mantle, and the cross-section is most sensitive to the mantle thickness.

Some preliminary estimates (see **Table**) of dielectric permittivity and thickness of mantles associated with craters of ~35 km (±1.5 km) in diameter were made with the model. Narrow range of diameters allows dealing with the similar ejecta volumes and similar excavation depth. This is important for tracing evolution of DDFs. As can be seen from the **Table** below, the mantle for DP craters is thicker than for CDH craters and FDH craters.

Craters type	**Mantle dielectric permittivity : thickness**
"Dark parabola" craters	3.1 ÷ 3.3 **:** 1 m ÷ 13 m 2.9 ÷ 3.1 **:** 10 m ÷ 13 m 3.8÷ 4.0 **:** 6 m ÷ 11 m
"Clear dark halo" craters	3.8 ÷ 4.0 **:** 2.5 m ÷ 5 m 3.6 ÷ 3.8 **:** 3 m ÷ 8 m 3.4 ÷ 4.0 **:** 0.2 m ÷ 1.2 m
"Faint dark halo" craters	3.3 ÷ 3.5 **:** < 0.5 m 3.8 ÷ 4.0 **:** < 0.7 m

Conclusions: In the frame of the model, the change of the radar contrast between the DDF and the surrounding surface can be treated as the decrease of the mantle thickness. This is in agreement with "dark parabola" - "clear dark halo" - "faint dark halo" sequence as a degradation sequence [4].

Our study shows that the analysis in radar cross-section – emissivity domain is promising for the study of surface mantles on Venus.

Acknowledgement. This work is partially supported by Finish Academy of Science.

References: [1] Campbell, D. et al. (1992) *JGR* **97**, 16249. [2] Arvidson, R.E. et al. (1992) *JGR* **97**, 13303. [3] Izenberg, N.R. et al. (1994) *GRL* **21**, No. 4, 289. [4] Basilevsky, A.T. and J.W. Head. (2002) *JGR* **107**, 10.1029/2001JE001584. [5] Ulaby, F.T. *et al.* (1986) *Microwave remote sensing: active and passive*, Artech House.